UNIVERSITY OF BATH
Department of Mechanical Engineering
FACULTY OF ENGINEERING AND DESIGN

FINAL YEAR MEng PROJECT
PROJECT SCOPING AND PLANNING

Name of the project: CFD Study of Cerebral Fusiform Aneurysms for Determining Patient-Specific Risk of Rupture

Your name: Romesh James Thayalan

Date of submission: 29th November 2023

Word count: 2480

Supervisor: *Dr Katharine Fraser*

Assessor: *Dr Lee Nissim*

CFD Study of Cerebral Fusiform Aneurysms for Determining Patient-Specific Risk of Rupture

November 28, 2023

Project Scoping and Planning Report

Romesh James Thayalan

University of Bath

Supervisor: Dr Katharine Fraser

Summary

Diagnosis of unruptured Intracranial Aneurysms (IAs) is becoming increasingly common as access to non-invasive imaging techniques rises. 3-13 % of these are fusiform (IFA) in shape which are characterised by dilations of the entire circumference of the cerebral vessel for a short distance. Rupture of IAs leads to Subarachnoid Haemorrhage (SAH) which has high mortality and morbidity rates. Intervention through open-skull surgery or endovascular treatment often carries risks equal to or greater than the risk of rupture and so understanding of the factors that lead to this is critical. However, understanding of this process remains poor. Haemodynamics is thought to play a central role by its interactions with the vessel wall mechanobiology. Therefore, there has been great interest in using Computational Fluid Dynamics (CFD) with geometry derived from patient scans to accurately quantify the haemodynamic environment in IAs. These are mainly focussed on the more common saccular intracranial aneurysm (SIA), however, meaning the haemodynamic factors behind IFAs are comparatively even less understood. There is little consensus as to what haemodynamic markers indicate an aneurysm that is likely to grow/rupture. Wall Shear Stress (WSS) is the principal candidate as it has been shown to have a direct effect on the Endothelial Cells (ECs) responsible for regulating inflammatory agent production at the artery walls thought to be linked to aneurysm growth and rupture. Most CFD studies of IAs make simplifying assumptions such as blood being a Newtonian fluid and use low order spatial and temporal discretisation schemes to solve the unsteady Navier-Stokes equations. The tortuous nature of the carotid siphon to the anterior circulation of the brain, has been shown to lead to weakly turbulent flow despite the modest Reynolds numbers involved (of the order $Re \approx 350$). The diffusing nature of IFAs introduces the possibility of greater flow instabilities being present while shear-thinning fluids are more resistant to transition than Newtonian fluids. Therefore, the present proposal aims to determine the effect of shear-thinning viscosity models on the flow instabilities in anterior IFAs from patient-specific Magnetic Resonance (MR) angiograms. Direct Numerical Simulations (DNS) with high order (second or greater) spatial and temporal discretisation schemes will be performed, first with steady inflow velocities, and then incorporating time-dependent pulsatile waveforms. The effects of rheological model on haemodynamic parameters such as WSS will be investigated alongside the flow instabilities present. The outcome of this research will be to determine whether the Newtonian viscosity model is sufficient to model the haemodynamics and weakly turbulent flow in IFAs of the anterior circulation.

List of Acronyms

AAA Abdominal Aortic Aneurysm. 5, 6

ACA Anterior Cerebral Artery. 7

AWE Aneurysm Wall Enhancement. 4

CFD Computational Fluid Dynamics. 1, 3, 4, 6, 7, 9, 10

CT Computed Tomography. 3

DNS Direct Numerical Simulation. 1, 5, 9

EC Endothelial Cell. 1, 5

fKE Fluctuating Kinetic Energy. 9

GP Generalised Power law. 4

IA Intracranial Aneurysm. 1, 3, 4, 7, 9

ICA Internal Carotid Artery. 5, 7–9

IFA Intracranial Fusiform Aneurysm. 1, 3–7, 10, 11

MCA Middle Cerebral Artery. 7

MR Magnetic Resonance. 1, 4, 7, 10

MRI Magnetic Resonance Imaging. 3, 4

OSI Oscillatory Shear Index. 9

PHASES Population-Hypertension-Age-Size of Aneurysm-Earlier SAH-Site. 3

SAH Subarachnoid Haemorrhage. 1–3

SIA Saccular Intracranial Aneurysm. 1, 3–5, 10

VA Vertebral Artery. 6

VFR Volume Flow Rate. 8

VMTK Vascular Modelling Toolkit. 7, 10

WSS Wall Shear Stress. 1, 4–6, 9

1 Background

The increased availability of non-invasive neuroradilogical techniques such as Computed Tomography (CT) and Magnetic Resonance Imaging (MRI) has led to the rise in the discovery of unruptured Intracranial Aneurysms (IAs) [1, 2]. Approximately 1 % of these rupture annually which has extremely serious effects of Subarachnoid Haemorrhage (SAH), associated with high mortality and morbidity [3]. Most IAs are saccular (SIA), which are pouch-like pathological dilations of the aneurysm wall (Figure 1(a)). 3-13 % are fusiform (IFA) [4], which are dilations involving the entire circumference for a short distance [5, 6]. Haemodynamics is thought to play a pivotal role in IA initiation, growth, and rupture, so for the last two decades there has been great interest in using patient angiograms to create patient-specific Computational Fluid Dynamics (CFD) models and generate a rupture-risk based on the patient's unique anatomy [3, 7]. Despite this, clinical decision-making makes no use of CFD whatsoever due to the lack of consensus on the links between haemodynamics and eventual rupture [7]. Instead, scoring rubrics such as PHASES are used based on trends seen in the population of aneurysms. These rubrics are not valid for IFAs and so their treatment is highly subjective, relying on continual monitoring - a growing IFA becoming a candidate for intervention [8]. Management of IFAs would therefore greatly benefit from patient-specific CFD simulations to understand the haemodynamics behind growth and rupture and to determine a reliable rupture risk [2, 3, 9].

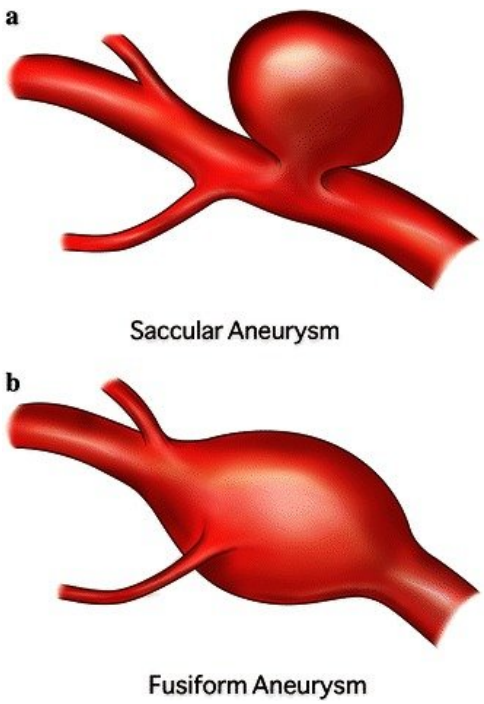

Figure 1: Representation of a saccular aneurysm (a), and a fusiform aneurysm (b) [10].

2 Literature Review

2.1 Haemodynamics' Links to Aneurysm Mechanobiology

Early *in vitro* works by Roach et al. [11] on saccular bifurcation aneurysms of the circle of Willis linked shear rate to degeneration of the internal elastic lamina and a weakening of the aneurysm wall. It was also determined that blood flow exhibited transitional features that caused this damage [12] and that non-Newtonian viscosity effects were influential in slow regions [13]. Since transition and non-Newtonian effects were initially computationally prohibitive, and the majority of IAs are saccular, the early CFD works focussed on low (first) order discretisation and non-Newtonian models of SIAs, which found that high WSS was linked to rupture [14, 15, 16].

More recently, CFD studies have been conducted on IFAs. Raghuram et al. [17] conducted pulsatile, Newtonian simulations on IFAs and SIAs imaged with high-resolution MRI. They took inflow rates from a study of healthy subjects [18] without scaling by the artery diameter, however, shown to introduce errors in WSS by Chnafa et al. [19]. Areas of lumen that exhibit Aneurysm Wall Enhancement (AWE), where the ratio of signal intensity of the aneurysm wall to contrast ratio of the pituitary stalk is large, coincided with areas of low WSS. AWE has been associated with increased risk of rupture for IFAs by the same group [20] and Peng et al. [21, 22].

Jou et al. [23] followed two patients with basilar IFAs acquiring patient-specific lumenal geometry, inflow and outflow rates using MR angiography and velocimetry. Newtonian simulations were performed, which showed very low WSS on the inferior aspect of one patient's aneurysm which grew significantly over the monitoring period.

2.2 Rheological Modelling

From comparisons of *in vitro* tests and numerical simulations, the dominant non-Newtonian behaviour exhibited by intracranial blood flow is shear-thinning [24]. This can be modelled by laws such as Carreau, Casson, Generalised Power law (GP), K-L, and Cross as Figure 2 shows.

Saqr et al [25] discovered evidence for non-Newtonian behaviour in intracranial vessels from Doppler ultrasonography measurements. Several CFD studies have been conducted to determine the effect of shear-thinning rheology on salient parameters such as WSS with highly varying results.

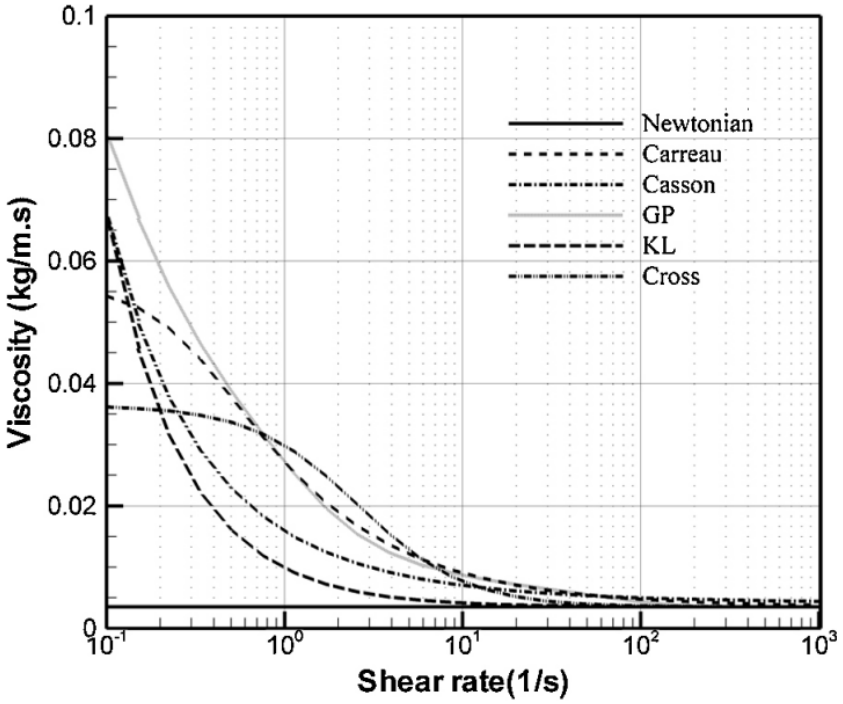

Figure 2: Variation of dynamic viscosity with shear rate for the different shear-thinning models of blood and the Newtonian viscosity model.

Lee and Steinman [26] simulated flow in healthy Internal Carotid Arteries (ICAs) showing modest WSS changes compared to geometric uncertainty. By contrast a study on ICAs with SIAs by Xiang et al [27] found a large overprediction of WSS in low WSS regions by the Newtonian model as did Castro et al [28]. Khan et al. [29] showed, however, that the order of spatial and temporal discretisation had a larger impact than rheology model. They did admit that in areas where thrombosis is possible, such as in IFAs [30], shear-thinning effects may not be negligible. Indeed, Rayz et al. [31] discovered that the low-velocity regions of a giant basilar IFA had better agreement with subsequent thrombosed regions when using a shear-thinning model. Comparisons of rheology models in a simplified fusiform Abdominal Aortic Aneurysm (AAA) by Ma and Turan [32] showed significant WSS differences at the proximal and distal ends.

2.3 Flow Instabilities in Aneurysmal Flow

It has been established from *in vitro* experimetns that Endothelial Cells (ECs) which line the internal artery walls respond to laminar flow by suppressing inflamation, and to disturbed flow by upregulating inflammatory agents, which is linked to aneurysm growth and rupture [33, 34]. Direct Numerical Simulation (DNS) results of a stenosed ICA showed weakly turbulent fluctuations in pressure and velocity in the poststenotic region, which has an expanding geometry similar to the entrance of an IFA.

This study assumed a Newtonian viscosity based on Lee and Steinman [26], which was concerned with healthy vessels, without the expanding geometry causing disturbed flow. Shear-thinning fluids have been shown experimentally to undergo delayed transition when compared to Newtonian fluids [35]. From numerical studies, recirculation zone lengths in backward-facing steps have also been shown to decrease when modelling blood as shear-thinning [36, 37]. A CFD study of a fusiform AAA assuming Newtonian viscosity demonstrated a recirculation zone at the proximal expansion [38], the geometry of which is analogous to a backward-facing step (Figure 3). It is therefore possible that the Newtonian viscosity model may overpredict recirculation zone length and hence the intra-aneurysmal haemodynamics in IFAs.

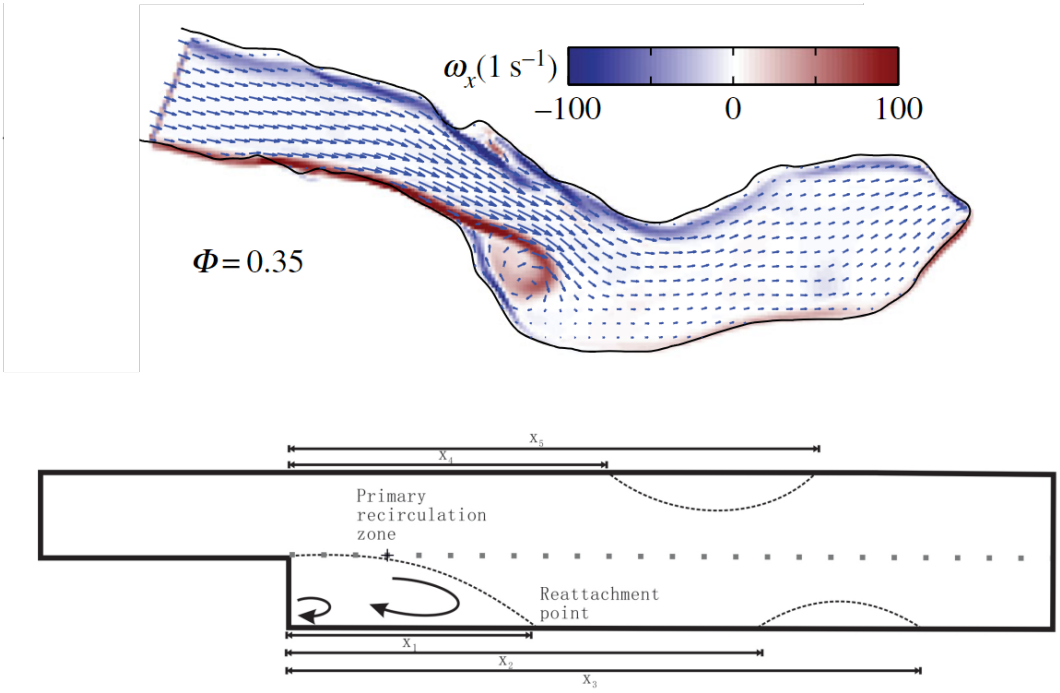

Figure 3: Comparison of the midplane of the AAA simulated by Poelma et al. [38] showing velocity vectors and vorticity, and a backward facing step with recirculation zone [37].

The study investigating shear-thinning modelling in IFAs by Rayz et al. [31] only considers basilar arteries which is in the posterior circulation of the brain. The anterior circulation has a much more tortuous route to the brain, through the carotid siphon with sharp bends and large area changes, than the posterior circulation, which has a straight and direct path from the aorta through the Vertebral Arteries (VAs). High-resolution CFD performed by Valen-Sendstad et al. [39] of the carotid siphon showed three of five cases had mild to high instabilities at peak systole. Given the link between disturbed flow and endothelial dysfunction [34], and the effect shear-thinning rheology has on this [35, 36, 37], a high-resolution numerical study of anterior circulation IFAs is needed to determine what effect shear-thinning rheology has on intra-aneurysmal flow instabilities and hence haemodynamic parameters such as WSS.

3 Aims and Objectives

The aim of this study will be to determine the effect of shear-thinning rheology on the transitional flow instabilities and haemodynamics in intracranial fusiform aneurysms of the anterior circulation.

To reach this aim, the following objectives must be achieved:

Objective 1 — Construct vascular models from MR angiograms to obtain geometry and estimate inflow and outflow rates for the computational models.

Objective 2 — Use CFD models to compare the differences in flow instabilities and hameodynamics in IFAs between Newtonian and shear-thinning rheologies under estimated steady inflow rate.

Objective 3 — Incorporate estimated pulsatile inflow velocities into the CFD model to compare flow instabilities and hameodynamics between Newtonian and shear-thinning rheologies, and the relative differences compared to the steady inflow simulations.

Objective 4 ***(extension, time permitting)*** — Construct CFD models of saccular IA(s) and/or healthy vessels and compare the effects of rheology model to its effects in IFAs.

4 Workplan

To achieve the objectives, the project will be divided into four Work Packages (**WP**s):

WP1 — Construct Vascular Models and Estimate Boundary Conditions

MR angiograms of IFAs have been sourced from the open-source dataset provided by di Noto et al. [40]. To achieve **Objective 1**, these must be pre-processed for meshing (**T1.1**). Additionally, the inlet conditions must be estimated (**T1.2**).

T1.1 *Perform Segmentations of MR Angiograms*

Three IFAs will be selected aiming to have one from the three main anterior arteries – the ICA, MCA, and Anterior Cerebral Artery (ACA). They will be labelled sub-a,b,c. These will be segmented at the most proximal point of the ICA so flow instabilities in the carotid siphon to be captured [39, 41]. SimVascular will be used as it has extensive documentation and tutorials. If this process takes longer than expected, this will be mitigated by (**M1.1.1**) reducing the number of vessels studied. The geometries will have cylindrical extensions added to inlets and outlets to ensure fully developed flow. Should SimVascular prove to not be appropriate, (**M1.1.2**) the Vascular Modelling Toolkit (VMTK) will be used, as it is also open-source and has been used in previous studies [17]. Failing this, segmentation can be performed in MATLAB using the Medical Imaging Toolbox (**M1.1.3**).

T1.2 *Estimate Inflow and Outflow Boundary Conditions*

The cycle-averaged inflow rates, Q, can be estimated by

$$Q(ml/s) = 21.2 \cdot D^2(cm), \tag{1}$$

from measurements made by Valen-Sendstad et al. [42]. This was shown to be more accurate for intracranial flow than Murray's law by Chnafa et al. [19]. A low and high value for inflow rate will be estimated by linearly scaling the estimated value for an inflow rate sensitivity study.

From Q, the peak flow rate, Q_{peak}, can be calculated by

$$Q_{peak} = 1.6 \cdot Q + 0.25ml/s, \tag{2}$$

from Ford et al. [18]. These values can then be mapped to feature points in VFR waves they measured (Figure 4) for the pulsatile inlet conditions. Low and high peak waveforms can then be generated for the pulsatility sensitivity study. If this approach is not easily implemented, a sine wave can be used to approximate pulsatile flow (**M1.2.1**). For a heartrate of 75 bpm, and mean ICA diameter of 4.1 mm, the Womersley number, $\alpha \approx 6.32$, so a Womersley velocity profile should be applied [39].The outflow rates can be modelled as traction-free outlets as is commonly done in previous studies [16, 17].

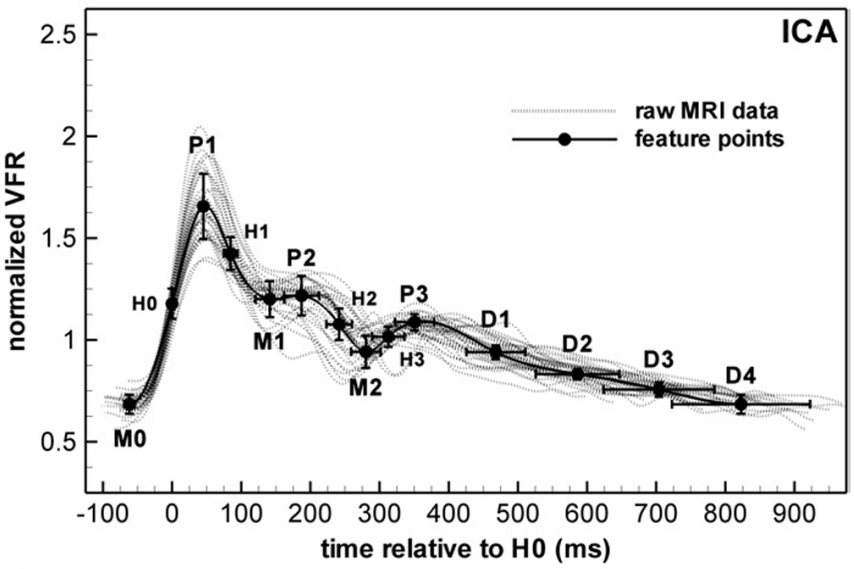

Figure 4: Volume Flow Rate (VFR) normlalised by cycle averaged VFR against time relative to the H0 feature point from PC-MRI measurements.

WP2 — Conduct CFD Simulations Under Steady Inlet Conditions

To accurately model the flow instabilities present in IAs, high-order spatial and temporal discretisation schemes for DNS is required [39, 43, 44]. To do this, the University of Bath cloud supercomputer, Nimbus, should be used. For a project of this scale, a element limit of the order $\sim 10 \times 10^6$ is deemed sensible. The average Reynolds number in the ICA is $Re \approx 363$ [39], and the number of elements required to resolve all turbulence scales, $N \approx Re^{9/4}$ [45], giving a required number of elements of approximately 0.575×10^6. High-resolution studies have used $2.6\text{–}3 \times 10^6$ elements [39, 44], however, which still lies within the 10×10^6 limit.

To achieve **Objective 2**, the vascular models must be discretised, and a grid and timestep independence study conducted (**T2.1**) under a Newtonian viscosity model. Post-processing setup will be carried out concurrently (**T2.2**). Sensitivity to inflow rate will be assessed for the three cases with a Newtonian viscosity model (**T2.3**). A shear-thinning viscosity model will then be applied and the results of each model compared (**T2.4**).

T2.1 *Discretise Vascular Models and Ensure Grid and Timestep Independence*

A base grid will be generated in Ansys Meshing. A coarse and fine mesh will be prepared for each. The grids will be solved using Ansys CFX. For each case, monitors of average WSS, and aneurysm averaged Fluctuating Kinetic Energy (fKE) will be set up to determine convergence and grid independence [31, 44]. Time-step independence will be ensured. If this process takes longer than anticipated, grid and time-step independence can be determined for a single subject (**M2.1.1**).

T2.2 *Post-Processing Setup*

While the grid and time-step independence studies are running, the post-processing codes can be set up. User-functions such as Oscillatory Shear Index (OSI), plots of WSS and fKE in Ansys CFD Post. MATLAB code will be written to compute power spectral density distributions to determine flow instabilities. The post-processing will be made generalised such that it can be used for all simulations.

T2.3 *Steady Inflow Sensitivity Study*

For each subject, all inflow rates will be simulated and the effects on WSS, fKE, and power spectral density distributions will be determined. If there is not enough time to do this for each case, the sensitivity analysis will be performed for a single subject (**M2.3.1**).

T2.4 *Compare the Results of Newtonian and Shear-Thinning Viscosity Models*

The shear-thinning viscosity model will be set up and simulations run for each inflow rate if sensitivity is high and time permits (**M2.4.1**). The flow stability and haemodynamic parameters will be compared between the viscosity models [44].

WP3 — Conduct CFD Simulations Under Pulsatile Inlet Conditions

To achieve **Objective 3**, simulations will be performed using the pulsatile inlet conditions estimated from **WP1** with the solution strategy from **WP2**. First a sensitivity study to pulsatile inflow conditions **T3.1** for the Newtonian model will be performed, and then comparing these results to those from the shear-thinning model **T3.2**.

T3.1 *Pulsatile Inflow Sensitivity Study*

For each case, the different pulsatile profiles will be run and the flow stability and haemodynamic parameters will be compared. If there is insufficient time to do this, the sensitivity study will be performed for a single case (**M3.1.1**), or it can be omitted (**M3.1.2**).

T3.2 *Compare the Results of Newtonian and Shear-Thinning Viscosity Models*

The shear-thinning viscosity model will be set up for each inflow profile if sensitivity is high and time allows (**M3.2.1**). The flow stability and haemodynamic parameters will be compared for the pulsatile case and the relative differences to the steady inflow cases will be analysed.

WP4 (*Optional*) — Effect of Shear-Thinning on SIA/Healthy Vessels vs. IFAs

If there is significant time left after completing **WP1**–**3**, the same analysis will be performed on SIAs/healthy vessels. To meet **Objective 4**, SIAs and/or healthy versions of the same vessels should be pre-processed and their inlet and outlet conditions determined (**T4.1**). Pulsatile inlet simulations will be performed using a Newtonian and a shear-thinning model. The effects of rheological model on haemodynamics will be compared to the effects seen from pulsatile IFA simulations from **WP3** (**T4.2**).

T4.1 *Pre-Processing and Definition of Boundary Conditions*

Vessels from the same as investigated for IFAs with SIAs or no diseases will be selected and segmented using SimVascular. Similar to **WP1**, the MR angiograms will be segmented using SimVascular (or VMTK or MATLAB if required (**M4.1.1**)). The inflow conditions will be determined based on Equation 1.

T4.2 *Pulsatile Simulations of SIAs/Healthy Vessels with Newtonian and Shear-Thinning*

Using the discretisation strategy developed in **WP2**, computational models of the SIAs and healthy vessels will be made in Ansys Meshing and CFX. Pulsatile simulations will then be run with Newtonian and shear-thinning models.

T4.3 *Comparison of the Effect of Rheological Model on SIAs and Healthy Vessels vs. IFAs*

The post-processing tools made in **WP2** will be used to characterise the differences in haemodynamics due to rheological models. These will be compared to existing studies. The relative differences

compared to those caused in IFAs can then be determined.

Overleaf is a Project Plan outlining how the project will be achieved. Letters denote a task being completed for the corresponding subject (a, b, or c).

Project Plan

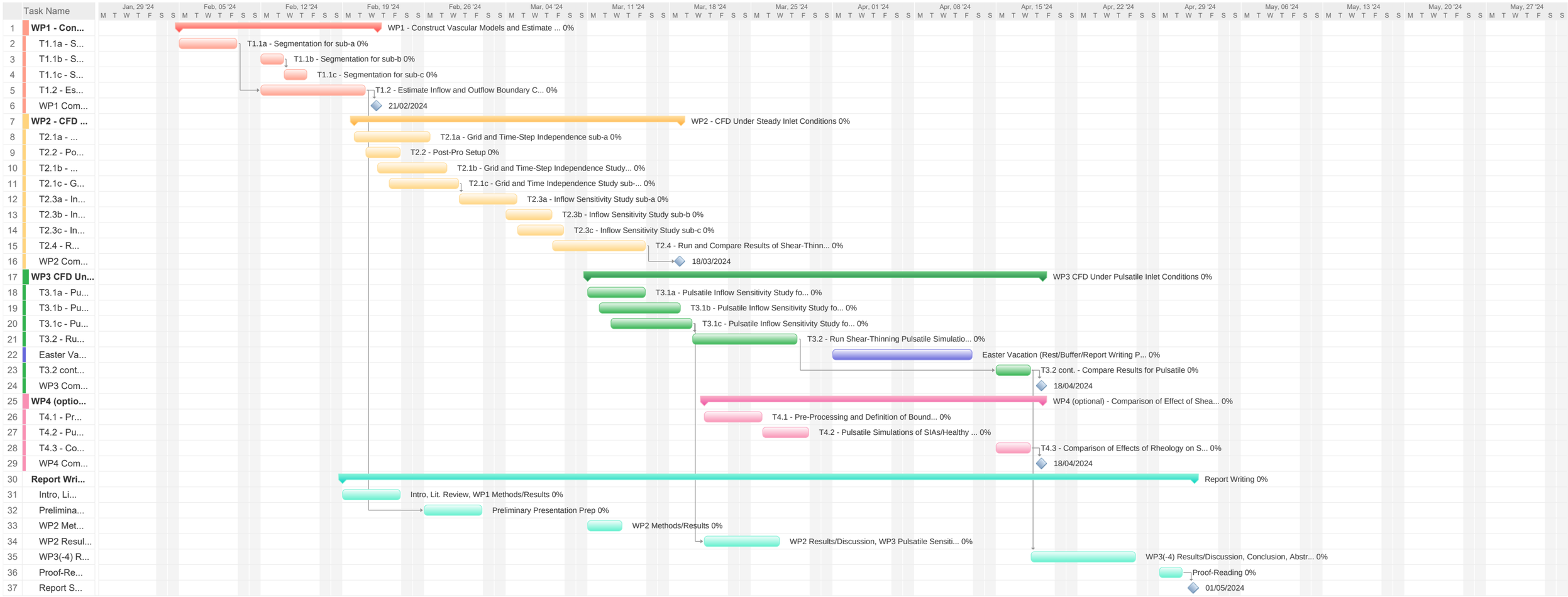

References

[1] M. H. M. Vlak, A. Algra, R. Brandenburg, and G. J. E. Rinkel, "Prevalence of unruptured intracranial aneurysms, with emphasis on sex, age, comorbidity, country, and time period: a systematic review and meta-analysis," *Lancet neurology*, vol. 10, no. 7, pp. 626–636, 2011.

[2] D. O. Wiebers, "Unruptured intracranial aneurysms: natural history, clinical outcome, and risks of surgical and endovascular treatment," *Lancet*, vol. 362, no. 9378, pp. 103–111, 2003.

[3] D. M. Sforza, C. M. Putman, and J. R. Cebral, "Hemodynamics of cerebral aneurysms," *Annual review of fluid mechanics*, vol. 41, no. 1, pp. 91–107, 2009.

[4] M. Al-Yamany and I. B. Ross, "Giant fusiform aneurysm of the middle cerebral artery: successful hunterian ligation without distal bypass," *British journal of neurosurgery*, vol. 12, no. 6, pp. 572–575, 1998.

[5] S.-H. Park, M.-B. Yim, C.-Y. Lee, E. Kim, and E.-I. Son, "Intracranial fusiform aneurysms: It's pathogenesis, clinical characteristics and managements," *Journal of Korean Neurosurgical Society*, vol. 44, no. 3, pp. 116–123, 2008.

[6] J. M. Findlay, C. Hao, and D. Emery, "Non-atherosclerotic fusiform cerebral aneurysms," *Canadian journal of neurological sciences*, 2002.

[7] K. M. Saqr, S. Rashad, S. Tupin, K. Niizuma, T. Hassan, T. Tominaga, and M. Ohta, "What does computational fluid dynamics tell us about intracranial aneurysms? a meta-analysis and critical review," *Journal of Cerebral Blood Flow and Metabolism*, vol. 40, no. 5, pp. 1021–1039, 2020. [Online]. Available: <GotoISI>://WOS:000527794300010

[8] J. Moon, Y. D. Cho, D. H. Yoo, J. Lee, H.-S. Kang, W.-S. Cho, J. E. Kim, L. Zhang, and M. H. Han, "Growth of asymptomatic intracranial fusiform aneurysms: Incidence and risk factors," *Clinical neuroradiology (Munich)*, vol. 29, no. 4, pp. 717–723, 2019.

[9] A. H. Siddiqui, A. A. Abla, P. Kan, T. M. Dumont, S. Jahshan, G. W. Britz, L. N. Hopkins, and E. I. Levy, "Panacea or problem: flow diverters in the treatment of symptomatic large or giant fusiform vertebrobasilar aneurysms," *Journal of Neurosurgery*, vol. 116, no. 6, pp. 1258–1266, 2012. [Online]. Available: <GotoISI>://WOS:000304294000020

[10] K. Withers, G. Carolan-Rees, and M. Dale, "Pipeline™ embolization device for the treatment of complex intracranial aneurysms: A nice medical technology guidance," *Applied health economics and health policy*, vol. 11, no. 1, pp. 5–13, 2013.

[11] M. R. Roach, S. Scott, and G. G. Ferguson, "The hemodynamic importance of the geometry of bifurcations in the circle of willis (glass model studies)," *Stroke (1970)*, vol. 3, no. 3, pp. 255–267, 1972.

[12] G. G. Ferguson, "Turbulence in human intracranial saccular aneurysms," *Journal of neurosurgery*, 1970.

[13] H. J. Steiger, A. PollL, D. Liepsch, and H.-J. Reulen, "Haemodynamic stress in lateral saccular aneurysms: an experimental study," *Acta neurochirurgica*, vol. 86, no. 3-4, pp. 98–105, 1987.

[14] J. R. Cebral, M. A. Castro, J. E. Burgess, R. S. Pergolizzi, M. J. Sheridan, and C. M. Putman, "Characterization of cerebral aneurysms for assessing risk of rupture by using patient-specific computational hemodynamics models," *American Journal of Neuroradiology*, vol. 26, no. 10, pp. 2550–2559, 2005.

[15] J. R. Cebral, M. A. Castro, D. Millan, A. F. Frangi, and C. Putman, "Pilot clinical study of aneurysm rupture using image-based computational fluid dynamics models," in *Proc. SPIE*, vol. 5746, no. 1. SPIE, 2005, pp. 245–256.

[16] M. Castro, C. Putman, A. Radaelli, A. Frangi, and J. Cebral, "Hemodynamics and rupture of terminal cerebral aneurysms," *Academic Radiology*, vol. 16, no. 10, pp. 1201–1207, 2009. [Online]. Available: https://www.sciencedirect.com/science/article/pii/S1076633209002578

[17] A. Raghuram, A. Galloy, M. Nino, S. Sanchez, D. Hasan, S. Raghavan, and E. A. Samaniego, "Comprehensive morphomechanical analysis of brain aneurysms," *Acta neurochirurgica*, vol. 165, no. 2, pp. 461–470, 2023.

[18] M. D. Ford, N. Alperin, S. H. Lee, D. W. Holdsworth, and D. A. Steinman, "Characterization of volumetric flow rate waveforms in the normal internal carotid and vertebral arteries," *Physiological measurement*, vol. 26, no. 4, pp. 477–488, 2005.

[19] C. Chnafa, "Errors in power-law estimations of inflow rates for intracranial aneurysm cfd," *Journal of Biomechanics*, vol. 80, pp. 159–166, 2018.

[20] A. Raghuram, S. Sanchez, L. Wendt *et al.*, "3d aneurysm wall enhancement is associated with symptomatic presentation," *Journal of neurointerventional surgery*, pp. neurintsurg–2022–019 125, 2022.

[21] F. Peng, M. Fu, J. Xia *et al.*, "Quantification of aneurysm wall enhancement in intracranial fusiform aneurysms and related predictors based on high-resolution magnetic resonance imaging: a validation study," *Therapeutic advances in neurological disorders*, vol. 15, pp. 175 628 642 211 053–17 562 864 221 105 342, 2022.

[22] F. Peng, H. Niu, X. Feng *et al.*, "Aneurysm wall enhancement, atherosclerotic proteins, and aneurysm size may be related in unruptured intracranial fusiform aneurysms," *European radiology*, vol. 33, no. 7, pp. 4918–4926, 2023.

[23] L.-D. Jou, G. Wong, B. Dispensa, M. T. Lawton, R. T. Higashida, W. L. Young, and D. Saloner, "Correlation between lumenal geometry changes and hemodynamics in fusiform intracranial aneurysms," *American Journal of Neuroradiology*, vol. 26, no. 9, pp. 2357–2363, 2005.

[24] F. J. H. Gijsen, F. N. van de Vosse, and J. D. Janssen, "The influence of the non-newtonian properties of blood on the flow in large arteries: steady flow in a carotid bifurcation model," *Journal of biomechanics.*, vol. 32, no. 6, pp. 601–608, 1999.

[25] K. M. Saqr, O. Mansour, S. Tupin, T. Hassan, and M. Ohta, "Evidence for non-newtonian behavior of intracranial blood flow from doppler ultrasonography measurements," *Medical biological engineering computing*, vol. 57, no. 5, pp. 1029–1036, 2019.

[26] S. W. Lee and D. A. Steinman, "On the relative importance of rheology for image-based cfd models of the carotid bifurcation," *Journal of Biomechanics*, vol. 39, p. S283, 2006.

[27] J. Xiang, M. Tremmel, J. Kolega, E. I. Levy, S. K. Natarajan, and H. Meng, "Newtonian viscosity model could overestimate wall shear stress in intracranial aneurysm domes and underestimate rupture risk," *Journal of neurointerventional surgery*, vol. 4, no. 5, pp. 351–357, 2012.

[28] M. A. Castro, M. C. A. Olivares, and J. R. Cebral, "Hemodynamic differences in intracranial anerusysm blebs due to blood rheology," *Journal of Physics: Conference Series*, vol. 477, no. 1, pp. 1–10, 2013.

[29] M. O. Khan, D. A. Steinman, and K. Valen-Sendstad, "Non-newtonian versus numerical rheology: Practical impact of shear-thinning on the prediction of stable and unstable flows in intracranial aneurysms," *International journal for numerical methods in biomedical engineering*, vol. 33, no. 7, p. n/a, 2017.

[30] R. D. Brownlee, B. I. Tranmer, R. J. Sevick, G. Karmy, and B. J. Curry, "Spontaneous thrombosis of an unruptured anterior communicating artery aneurysm; an unusual cause of ischemic stroke," *Stroke (1970)*, vol. 26, no. 10, pp. 1945–1949, 1995.

[31] V. Rayz, L. Boussel, M. Lawton, G. Acevedo-Bolton, L. Ge, W. Young, R. Higashida, and D. Saloner, "Numerical modeling of the flow in intracranial aneurysms: Prediction of regions prone to thrombus formation," *Annals of biomedical engineering*, vol. 36, no. 11, pp. 1793–1804, 2008.

[32] J. Ma and A. Turan, "Pulsatile non-newtonian haemodynamics in a 3d bifurcating abdominal aortic aneurysm model," *Computer methods in biomechanics and biomedical engineering*, vol. 14, no. 8, pp. 683–694, 2011.

[33] J. S. Hudson, D. S. Hoyne, and D. M. Hasan, "Inflammation and human cerebral aneurysms: current and future treatment prospects," *Future neurology*, 2013.

[34] J.-J. Chiu and S. Chien, "Effects of disturbed flow on vascular endothelium: pathophysiological basis and clinical perspectives," *Physiological reviews*, vol. 91, no. 1, pp. 327–387, 2011.

[35] D. Biswas, D. M. Casey, D. C. Crowder, D. A. Steinman, Y. H. Yun, and F. Loth, "Characterization of transition to turbulence for blood in a straight pipe under steady flow conditions," *Journal of biomechanical engineering*, vol. 138, no. 7, 2016.

[36] H. W. Choi and A. I. Barakat, "Numerical study of the impact of non-newtonian blood behavior on flow over a two-dimensional backward facing step," *Biorheology (Oxford)*, vol. 42, no. 6, pp. 493–509, 2005.

[37] N. S. Kelly, H. S. Gill, A. N. Cookson, and K. H. Fraser, "Influence of shear-thinning blood rheology on the laminar-turbulent transition over a backward facing step," *Fluids (Basel)*, vol. 5, no. 2, p. 57, 2020.

[38] C. Poelma, P. N. Watton, and Y. Ventikos, "Transitional flow in aneurysms and the computation of haemodynamic parameters," *Journal of the Royal Society interface*, vol. 12, no. 105, p. 20141394, 2015.

[39] K. Valen-Sendstad, M. Piccinelli, and D. A. Steinman, "High-resolution computational fluid dynamics detects flow instabilities in the carotid siphon: Implications for aneurysm initiation and rupture?" *Journal of biomechanics*, vol. 47, no. 12, pp. 3210–3216, 2014.

[40] T. Di Noto, G. Marie, S. Tourbier, Y. Alemán-Gómez, O. Esteban, G. Saliou, M. B. Cuadra, P. Hagmann, and J. Richiardi, "Towards automated brain aneurysm detection in tof-mra: Open data, weak labels, and anatomical knowledge," *Neuroinformatics (Totowa, N.J.)*, vol. 21, no. 1, pp. 21–34, 2023.

[41] M. A. Castro, C. M. Putman, and J. R. Cebral, "Computational fluid dynamics modeling of intracranial aneurysms: Effects of parent artery segmentation on intra-aneurysmal hemodynamics," *American Journal of Neuroradiology*, vol. 27, no. 8, pp. 1703–1709, 2006.

[42] K. Valen-Sendstad, M. Piccinelli, R. KrishnankuttyRema, and D. A. Steinman, "Estimation of inlet flow rates for image-based aneurysm cfd models: Where and how to begin?" *Annals of biomedical engineering*, vol. 43, no. 6, pp. 1422–1431, 2015.

[43] K. Valen-Sendstad and D. A. Steinman, "Mind the gap: impact of computational fluid dynamics solution strategy on prediction of intracranial aneurysm hemodynamics and rupture status indicators," *American journal of neuroradiology : AJNR*, vol. 35, no. 3, pp. 536–543, 2014.

[44] N. Varble, J. Xiang, N. Lin, E. Levy, and H. Meng, "Flow instability detected by high-resolution computational fluid dynamics in fifty-six middle cerebral artery aneurysms," *Journal of biomechanical engineering*, vol. 138, no. 6, pp. 061 009–061 009, 2016.

[45] H. K. H. K. Versteeg, *An introduction to computational fluid dynamics : the finite volume method*, 2nd ed. Harlow: Pearson Prentice Hall, 2007.